Electronic Supplementary Material (ESI) for Physical Chemistry Chemical Physics.

Reconciling Experimental and Theoretical Vibrational Deactivation in Low-Energy O+N_2 Collisions

Electronic Supporting Information

Qizhen Hong,[1,2] Massimiliano Bartolomei,[3] Fabrizio Esposito,[4] Cecilia Coletti,[5,a)] Quanhua Sun,[1,2] and Fernando Pirani[6]

[1)] *State Key Laboratory of High Temperature Gas Dynamics, Institute of Mechanics, Chinese Academy of Sciences, 100190 Beijing, China*

[2)] *School of Engineering Science, University of Chinese Academy of Sciences, Beijing 100049, China*

[3)] *Instituto de Física Fundamental - CSIC, C/ Serrano 123, Madrid, Spain*

[4)] *Consiglio Nazionale delle Ricerche, Istituto per la Scienza e Tecnologia dei Plasmi, Sede Secondaria di Bari, via Amendola 122/D 70126 Bari, Italy*

[5)] *Dipartimento di Farmacia, Università G. d'Annunzio Chieti-Pescara, via dei Vestini, 66100 Chieti, Italy.*

[6)] *Dipartimento di Chimica, Biologia e Biotecnologie, Università di Perugia, via Elce di Sotto, 8 - 06183 Perugia, Italy*

(Dated: 29 May 2021)

[a)] Electronic mail: ccoletti@unich.it

I. EXPERIMENTAL AND COMPUTATIONAL DETAILS

Ab-initio calculations of the O($^3\Pi$)-N$_2$($^1\Sigma_g^+$) intermolecular interaction energies have been carried out at the CCSD(T) level of theory by using the Molpro code[1] and the computed values have been corrected for the basis set superposition error by the counterpoise method of Boys and Bernardi[2]. The complete basis set (CBS) extrapolation of the obtained interaction energies has been performed by exploting the two-point correlation energy procedure of Halkier et al.[3,4] in conjuction with Dunning[5] augmented correlation-consistent aug-cc-pVQZ and aug-cc-pV5Z basis sets. For the analytical representation of the $^3\Pi$ and $^3\Sigma$ PESs we have considered that the sum of first two terms in Eq. 1 (V_{vdW}+V_{ct}) is globally accounted for with the sum of O-N atom-effective atom contributions, each one represented by an ILJ formula[6], while the last term (V_{el}) is described by a canonical expression of the quadrupole-quadrupole interaction, due to the non-negligible quadrupole moments of both monomers, and the related parameters are reported in Table S1. The internal coordinate dependence of both N_2 polarizability and quadrupole moment is taken from Refs.[7,8].

Molecular beam scattering experiments have been performed several years ago in the Perugia laboratory with an apparatus described in detail elsewhere[9]. In short, high angular and velocity resolution conditions were adopted in order to measure quantum *glory* interference effects, observable as an oscillatory pattern in the velocity dependence of the integral cross section $Q(v)$. A microwave discharge source operating at low pressure (few mbar) and temperature of about 10^3 K was used to generate the oxygen beam formed by atoms in their ground ^3P_J electronic state with a near statistical population of the spin orbit levels J=2,1,0. It has been also shown[10] that while J=2 and J=0 correlate at intermediate and short R with states of Π and Σ character, respectively, J=1 provides a combination of both; this assures that states of the two different symmetries are formed in a 2:1 statistical ratio during the scattering. The target gas formed by N_2 molecules was contained in a scattering chamber cooled at about 90 K. During the present analysis, which overcomes the previous one performed by a simple spherically symmetric potential model[9], cross sections are calculated from the present anisotropic intermolecular potential in the center of mass system within the semiclassical JWKB method and convoluted in the laboratory frame for a critical comparison with the experimental results. Taking into account that the rotational motion of molecules is cooled at about 90 K and that the proposed interaction is strongly anisotropic,

the infinite order sudden (IOS) approximation, that considers collisions occurring at fixed relative orientation of partners, is adopted.

A succinct desccription of the experimental determinations of vibrational deactivation rate coefficients follows: Eckstrom[11] measured vibrational relaxation time (estimated to have 50% uncertainty in the range 1200-3000 K) by shock-tube experiment, the ground state oxygen atoms were obtained from the shock-heated thermal dissociation of ozone and carbon monoxide was used as a tracer of vibrationally exited nitrogen due to fast energy exchange between these two species. The experimental data by Breshears and Bird[12] also used thermal decomposition of ozone to generate oxygen atoms in shock-tube experiment, in which a laser-beam deflection technique was used to derive the vibrational relaxation time (in the range 3000-4500 K) from the postshock density gradient. At lower temperatures (300-740 K), McNeal et al.[13] used a photo-ionization detector to measure the rate of vibrationally excited nitrogen in the afterglow. Unfortunately experimental results are unavailable for temperatures higher than 4500 K. The above original experimental data of vibrational relaxation time are then used to obtain the deexcitation rate coefficients from v=1 by means of the Bethe-Teller relation for vibrational energy exchange.

For the quantum-classical calculations[14] in this work (see the following), the lowest 9 vibrational states of N_2 are used and the initial state is v=1. The rates are computed at 47 initial values of total classical energy comprised between 50 cm^{-1} and 80000 cm^{-1}, with a more frequent sampling directed towards lower energies. For each energy value, 5000 trajectories were used, as well as an initial separation distance atom-diatom R equals to 50 Å and an impact parameter randomly chosen between 0 and 9 Å.

The probability of V-E transfer P_x is calculated according to the well-known Landau-Zener procedure[15–17]:

$$P_x = \exp\left(-\frac{2\pi H^2}{\hbar v_R \Delta}\right). \tag{1}$$

where v_R is the radial velocity at the crossing, Δ is the difference between the slope of the two PESs at the crossing point, here calculated to be Δ =0.7846 eV/Å. Note that only the collinear configuration is taken into account, as the most effective for inelastic processes. H is the coupling between the two PESs. In the range of collision energies associated to the temperature of interest here (below 10000 K), the use of a fixed value of H is sufficient to calculate reliable cross sections and rate coefficients. The exact determination of the

value of H is a complicated task. However, physical considerations allow to foresee that H should be comprised between 1-2 meV, a very small value, which in practice prevents its computation by ab-initio methods, as it falls within the accuracy of the highest available levels of theory. The coupling is expected to be small, because it occurs between two heterogeneous (i.e. corresponding to different Σ and Π symmetries) surfaces, which also ensures the validity of the Landau-Zener approach. Furthermore, H is the result of two contributions: the spin-orbit coupling, estimated to be slightly larger than in the O+Ar case[10] where the electrostatic contribution is absent, for which the first order non-adiabatic correction to adiabatic potential is around 0.2 meV, and the Coriolis coupling, which should be $\approx$ 1 meV, the value corresponding to a collision with an impact parameter of 1 Å at a relative velocity of 1.5 km/s[18]. A value of H= 1.5 meV was thus considered in the present calculation.

The radial velocity v_R at the crossing in eq. 1 is given by:

$$v_R^2 = \frac{2}{\mu}\left(E - \frac{\hbar^2(l+1)l}{2\mu R_c^2} - E_x\right), \tag{2}$$

in which l is the quantum number representing the orbital angular momentum of the collision complex (from 0 to $l_{\max}$, which guarantees v_R to be real), μ is the reduced mass and E is the collision energy (from 0 to 10 eV).

The cross section can then be computed from the P_x probability as

$$\sigma(E) = \frac{\pi}{k^2}\sum_{l=0}^{l_{\max}}(2l+1)\cdot 2\left(1-P_x\right)P_x, \tag{3}$$

in which P_x is the probability of the system staying on the same surface, and (1-P_x) is that of changing surface. Moreover, $k^2 = \frac{2\mu E}{\hbar^2}$. The rate coefficient for vibro-electronic energy transfer is obtained by

$$k_{V-E}(T) = \sqrt{\frac{8k_BT}{\pi\mu}}\frac{1}{(k_BT)^2}\int_0^\infty \sigma(E)e^{-E/k_BT}EdE. \tag{4}$$

II. THE IMPROVED LENNARD-JONES MODEL

For the analytical representation of the $^3\Pi$ and $^3\Sigma$ PESs, the sum of the first two components, $(V_{vdW} + V_{ct})$, has been formulated as the combination of pair interactions between

O (^{3}P) and each N atom of the N_2 molecule, represented by an Improved Lennard Jones (ILJ) function.

Specifically, $(V_{vdW} + V_{ct})$ is described as a sum of atom-"effective atom" contributions involving interaction pair-potentials between O (^{3}P) and each N atom of the N_2 molecule, i.e.,

$$V_{vdW} + V_{ct} = \sum_{i=1}^{2} V_{N_i-O}. \tag{5}$$

The contributions in the above equation depend on the "effective" electronic polarizability of the N atom within the N_2 molecule, which is different from that of the isolated N atom, and are described by an Improved Lennard Jones (ILJ) function[19], which depends on the distance R between the two interacting centers according to the expression:

$$V_{\mathrm{ILJ}}(R) = \varepsilon \left[\frac{6}{n(R)-6} \left(\frac{R_m}{R} \right)^{n(R)} - \frac{n(R)}{n(R)-6} \left(\frac{R_m}{R} \right)^{6} \right], \tag{6}$$

where ε and R_m (the related parameters are reported in Table S1) are the atom-effective atom interaction well depth and its location, respectively. This function gives a more realistic representation of both the repulsion and the long range attraction than the classic Lennard-Jones potential. The n term is expressed as a function of R:

$$n(R) = \beta + 4.0 \left(\frac{R}{R_m} \right)^2, \tag{7}$$

where β is a parameter which depends on the hardness of the interacting centers, and it is fixed to 8 in present cases.

Note that the differences in ε and R_m potential parameters associated to the two different symmetries, obtained following the guidelines reported in ref.[10], account for the electronic anisotropy of the O(^{3}P) atom in determining the bond stabilization by CT exclusively in the configuration $^3\Pi$.

III. THE QUANTUM-CLASSICAL METHOD

The quantum-classical method for atom-diatom collisions was introduced and developed by G.D. Billing[14] and is proven to be accurate and efficient to obtain cross sections and rate coefficients of heavy-impact processes involving vibrational energy transfer. The key feature

of this method is that the vibrational degrees of freedom are treated quantum mechanically, whereas the other degrees of freedom (the translational and the rotational motion) are treated classically. In order to handle with the whole system in a self-consistent way, the quantum mechanical degrees of freedom must evolve correctly under the influence of the surrounding classical motions. In turn, the classical degrees of freedom must respond correctly to quantum transitions.

According to the spirit of the quantum-classical method, vibration and rotational-vibrational coupling are treated quantum mechanically by close coupled equations. For atom-diatom collisions, there is just one quantum degree of freedom (the vibration of the diatom) and the total wavefunction is expanded in terms of the rotationally distorted Morse wave function $\phi_v(r,t)$ as follows:

$$\Psi(r,t) = \sum_v a_v(t)\phi_v(r,t)\exp\left(-\frac{itE_v}{\hbar}\right), \tag{8}$$

where r is the intramolecular distance of diatom, E_v is the eigenvalue of the rotationally distorted Morse wave functions $\phi_v(r,t)$ perturbed by rotational-vibrational coupling

$$\phi_v(r,t) = \phi_v^0(r) + \sum_{v'\neq v}\phi_{v'}^0(r)\frac{H_{v'v}}{E_v^0 - E_{v'}^0}, \tag{9}$$

where $H_{v'v}$ is the first-order centrifugal stretching term:

$$H_{v'v} = -j^2 m^{-1}\bar{r}^{-3} < \phi_{v'}^0 | r-\bar{r} | \phi_v^0 > \tag{10}$$

with j being the rotational momentum of the molecule and the operator $<>$ is obtained by integrating over r. ϕ_v^0 is the unperturbed eigenfunction of the Morse oscillator and E_v^0 is the eigenvalue approximated as

$$E_v^0 = \hbar\omega_e\left(v+\frac{1}{2}\right) - \hbar\omega_e x_e\left(v+\frac{1}{2}\right)^2 + \hbar\omega_e y_e\left(v+\frac{1}{2}\right)^3, \tag{11}$$

where ω_e is the oscillator wavenumber and x_e and y_e are the anharmonicity constants.

In order to obtain the amplitudes $a_{v'}$ for the inelastic processes $N_2(v)+O \rightarrow N_2(v')+O$, one then plugs the expansion (eq. 8) into the time-dependent Schrödinger equation and has to solve the following set of coupled equations for the amplitudes:

$$i\hbar\dot{a}_{v'}(t) = \sum_v\left[\left\langle\phi_{v'}^0\left|V(R,r,\gamma) + 2i\hbar j\frac{dj}{dt}\frac{\langle\phi_{v'}^0|(r-\bar{r})|\phi_v^0\rangle}{mr_{eq}^3(E_v^0 - E_{v'}^0)}\right|\phi_v^0\right\rangle\right]\cdot a_v(t)\exp\left[\frac{i}{\hbar}(E_{v'}-E_v)t\right], \tag{12}$$

in which the intermolecular potential $V(R, r, \gamma)$ is conveniently expressed as a function of R, the distance between the atom and the center of mass of the diatom and γ (the angle between r and R). The translational and rotational motions are obtained by solving the corresponding Hamilton equations by making use of an Ehrenfest averaged potential[20] defined as the quantum expectation value of the interaction potential. This mean-field method usually provides accurate quantum transition probabilities and properly conserves total (quantum plus classical) energy. A variable-order variable-step Adams predictor-corrector integrator[21] is then used to solve the coupled equations (eq. 12) and the classical equations of motion for rotation and translation. An absolute integration accuracy of 10^{-8} is achieved for all calculations in this work.

The vibrational wavefunction is initialized as a Morse wavefunction. The simultaneous propagation of the quantum and classical sets of equations produces the quantum transition amplitudes $a_{v'}$ which can be used to calculate cross sections for the vibrational transitions. The cross sections are obtained by averaging over a number of trajectories having randomly selected initial conditions, and a Monte Carlo average over the initial Boltzmann distribution of rotational energy is introduced to have rate coefficients for vibrational energy transfer. Thus an averaged cross section is defined as:

$$\sigma_{v\to v'}\left(T_0, \bar{U}\right) = \frac{\pi\hbar^4}{4\mu k_B^2 T_0^2 I} \int_0^{J_{\max}} \int_0^{j_{max}} \int_{l=|J-j|}^{J+j} dJdjdl \cdot (2J+1)\, P_{v\to v'}, \tag{13}$$

where μ is the reduced mass for the relative motion, J the total, j the rotational and l the initial orbital angular momentum. The moment of inertia is $I = mr^2$ and the temperature T_0 is arbitrary because it cancels out when calculating the rate coefficients. J_{max} and j_{max} are the upper limit for the randomly chosen total and rotational quantum numbers. Rate coefficients are then calculated through the following equation

$$k_{v\to v'}(T) = \left(\frac{8k_BT}{\pi\mu}\right)^{1/2} \left(\frac{T_0}{T}\right)^2 \int_0^{\infty} d\left(\frac{\bar{U}}{k_BT}\right) \cdot \exp\left(-\frac{\bar{U}}{k_BT}\right) \sigma_{v\to v'}\left(T_0, \bar{U}\right), \tag{14}$$

which holds for exothermic processes. $\bar{U}$, the symmetrized classical energy, is introduced to restore the detailed balance principle.[14,20]

Molecular parameters used in the present calculations are reported in Table S2.

Table S1: Parameters of the analytical formulation of the $^3\Pi$ and $^3\Sigma$ PESs for N_2 at its equilibrium distance (r_e=1.1007 Å). Note that parameters involved in the ILJ functions refer to atom - effective atom additive components.

	$^3\Pi$	$^3\Sigma$
	O-N interaction (ILJ formulation[6])	
ε (meV)	7.70	3.10
R_m (Å)	3.32	3.87
β	8	8
	quadrupole-quadrupole interaction	
Q_O (a.u)	0.475	-0.950
Q_{N_2} (a.u.)	-1.115	-1.115

Table S2: Molecular constants for N_2.

ω_e	2359.60 cm^{-1}
x_e	0.006126
y_e	0.0000032
r_{eq}	1.1007 Å
β	2.689 $Å^{-1}$
D_e	9.905 eV

Table S3: Rate coefficients for total vibrational relaxation of $N_2\left(^1\Sigma_g^+\right)(v=1)$ upon collision with $O\left(^3P\right)$ as a function of temperature.

T	V-T+V-E rates	Expt.[13]
300	1.05E-15	3.32E-15
460	9.95E-15	1.39E-14
640	3.22E-14	2.91E-14
740	4.83E-14	4.43E-14

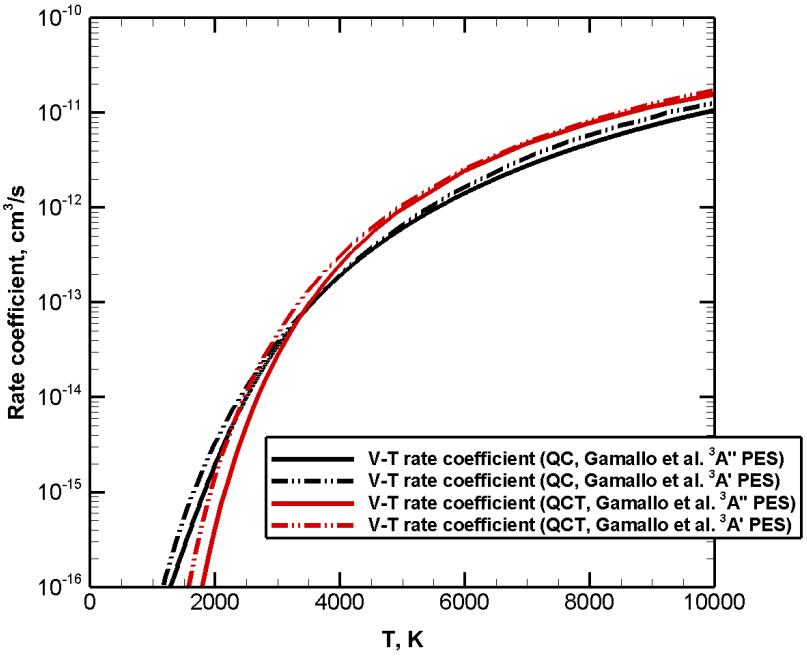

Figure S1: Rate coefficients for vibrational relaxation of $N_2(^1\Sigma_g^+)(v=1)$ upon collision with $O(^3P)$ as a function of temperature. V-T rate coefficients computed on Gamallo et al.[22] $^3A''$ (solid lines) and $^3A'$ PESs (dashed lines) by QCT[23] (red) and by the present QC (black) methods.

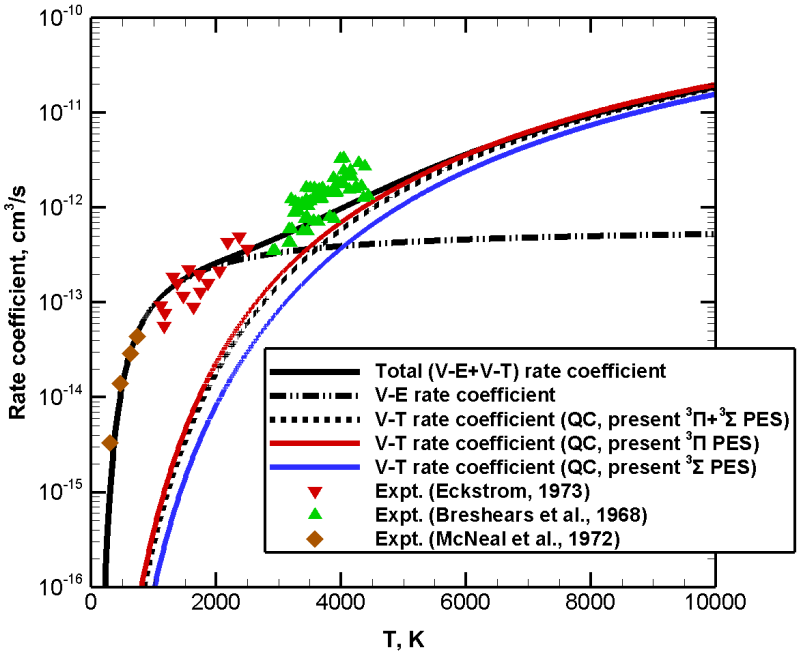

Figure S2: Rate coefficients for vibrational relaxation $N_2(^1\Sigma_g^+)(v = 1)$ upon collision with $O(^3P)$ as a function of temperature. Experimental data by Eckstrom[11] (red down triangles), by Breshears et al.[12] (green up triangles) and by McNeal[13] (brown diamonds) are reported together with QC V-T rate coefficients computed on the present $^3\Pi$ (red solid line) and $^3\Sigma$ (blue solid line): averaged (2:1) V-T rate coefficients are also reported (black dashed line), together with V-E (black dash-dot line) and total (V-T+V-E) vibrational relaxation rate coefficients (black solid line).

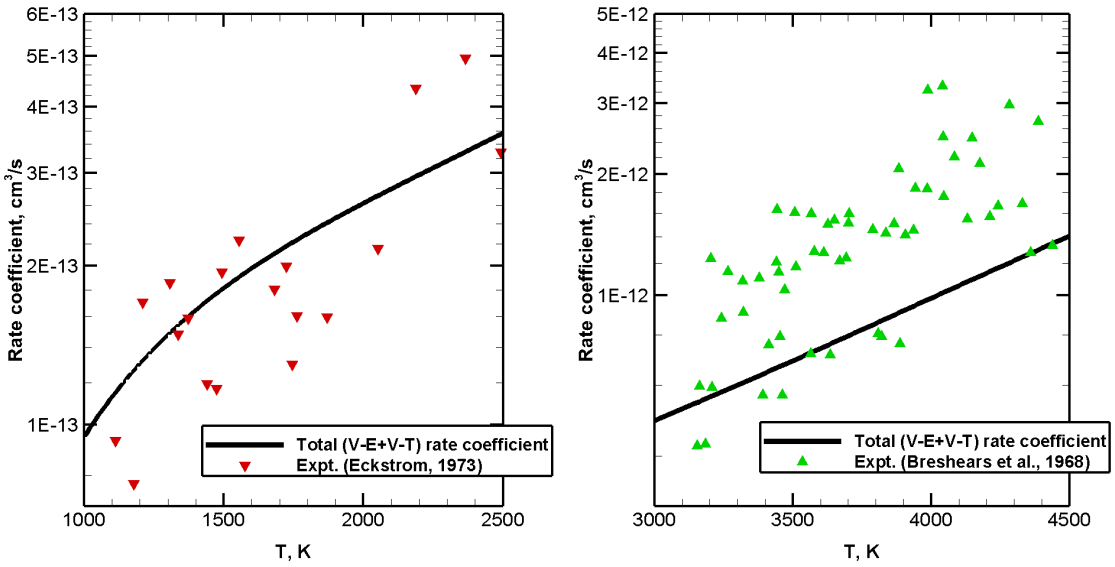

Figure S3: Calculated rate coefficients for vibrational relaxation $N_2(^1\Sigma_g^+)(v = 1)$ upon collision with $O(^3P)$ as a function of temperature in the 1000-2500 K range, left panel, and 3000-4500 K range, right panel. Experimental data by Eckstrom[11] (red down triangles) and by Breshears et al.[12] (green up triangles) are reported.

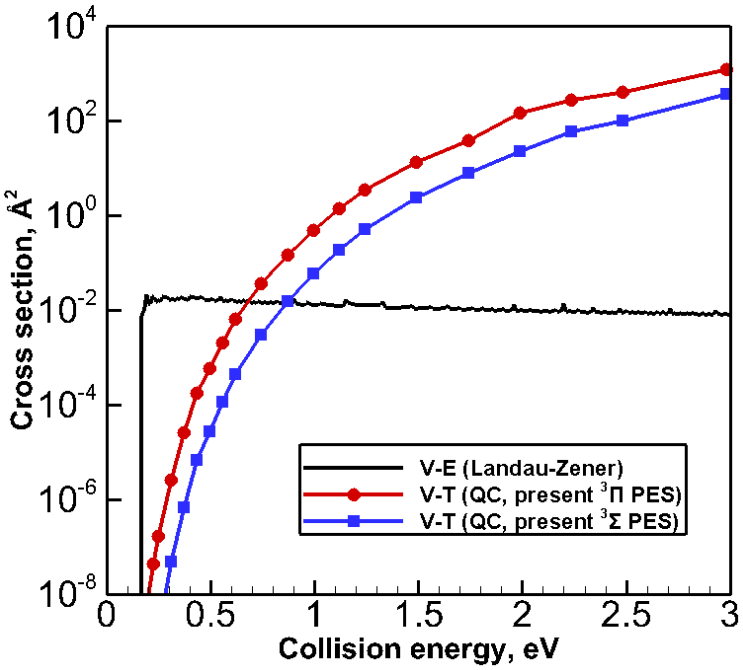

Figure S4: Cross sections for vibrational relaxation $N_2(^1\Sigma_g^+)(v = 1)$ upon collision with $O(^3P)$ as a function of collision energy. The QC V-T cross sections computed on the present $^3\Pi$ (red line with circle symbol) and $^3\Sigma$ (blue line with square symbol) are reported, together with V-E cross sections (black solid line).

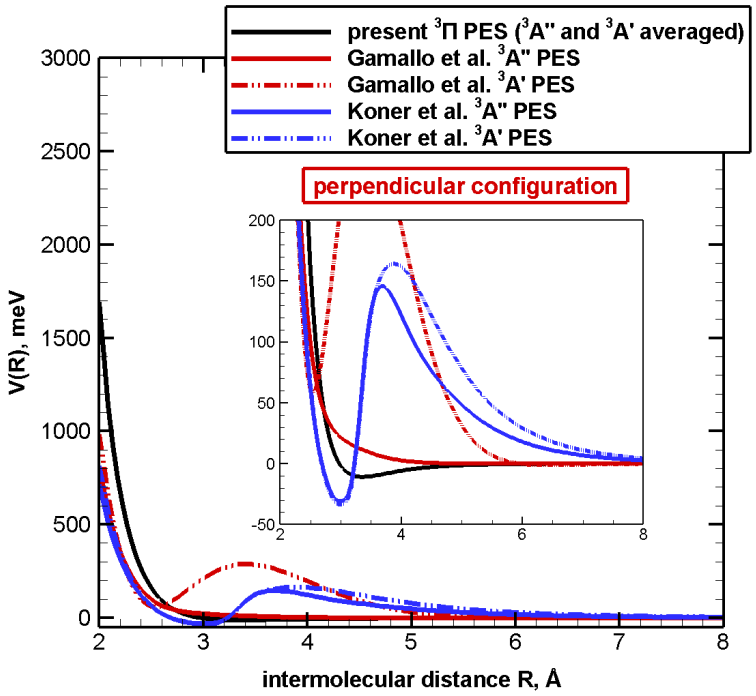

Figure S5: Behavior of different potential energy surfaces as a function of the intermolecular distance R for the perpendicular configuration, corresponding to the C_{2v} symmetry. The present $^3\Pi$ PES is reported as a solid black line, the Gamallo et al.[22] $^3A''$ and $^3A'$ are the red solid and dashed lines, respectively, and the Koner et al.[24] $^3A''$ and $^3A'$ are the blue solid and dashed lines, respectively.

REFERENCES

[1]H.-J. Werner, P. J. Knowles, R. Lindh, F. R. Manby, M. Schütz, P. Celani, T. Korona, G. Rauhut, R. D. Amos, A. Bernhardsson, A. Berning, D. L. Cooper, M. J. O. Deegan, A. J. Dobbyn, F. Eckert, C. Hampel, G. Hetzer, A. W. Lloyd, S. J. McNicholas, W. Meyer, M. E. Mura, A. Nicklass, P. Palmieri, R. Pitzer, U. Schumann, H. Stoll, A. J. Stone, R. Tarroni, and T. Thorsteinsson. Molpro, version 2012.1, a package of ab initio programs, 2012. see http://www.molpro.net.

[2]S.F. Boys and F. Bernardi. The calculation of small molecular interactions by the differences of separate total energies. some procedures with reduced errors. *Mol. Phys.*, 19:553–566, 1970.

[3]A. Halkier, T. Helgaker, P. Jorgensen, W. Klopper, H. Koch, J. Olsen, and A. K. Wilson. Basis-set convergence in correlated calculations on Ne, N_2, and H_2O. *Chem. Phys. Lett.*, 286:243–252, 1998.

[4]A. Halkier, T. Helgaker, P. Jorgensen, W. Klopper, J. Olsen, and A. K. Wilson. Basis-set convergence of the energy in molecular Hartree-Fock calculations. *Chem. Phys. Lett.*, 302:437–446, 1999.

[5]R. A. Kendall, T. H. Dunning, and R. J. Harrison. Electron affinities of the first-row atoms revisited. systematic basis sets and wave functions. *J. Chem. Phys.*, 96:6796–6806, 1992.

[6]F. Pirani, S. Brizi, L. Roncaratti, P. Casavecchia, D. Cappelletti, and F. Vecchiocattivi. Beyond the Lennard-Jones model: A simple and accurate potential function probed by high resolution scattering data useful for molecular dynamics simulations. *Phys. Chem. Chem. Phys.*, 10:5489–5503, 2008.

[7]D. Cappelletti, F. Pirani, B. Bussery-Honvault, L. Gómez, and M. Bartolomei. A bond-bond description of the intermolecular interaction energy: the case of weakly bound N_2-H_2 and N_2-N_2 complexes. *Phys. Chem. Chem. Phys*, 10:4281–4293, 2008.

[8]A. Lombardi, F. Pirani, Laganá, and M. Bartolomei. Energy transfer dynamics and kinetics of elementary processes (promoted) by gas-phase CO_2-N_2 collisions: Selectivity control by the anisotropy of the interaction. *J. Comput. Chem.*, 37:1463–1475, 2016.

[9]B. Brunetti, G. Liuti, E. Luzzatti, F. Pirani, and F. Vecchiocattivi. Study of the interactions of atomic and molecular oxygen with O_2 and N_2 by scattering data. *J. Chem. Phys.*, 74:6734–6741, 1981.

[10]V. Aquilanti, R. Candori, and F. Pirani. Molecular beam studies of weakly interactions for open shell systems: The ground and the lowest excited states of rare gas oxides. *J. Chem. Phys.*, 89:6157–6164, 1988.

[11]D. J. Eckstrom. Vibrational relaxation of shock-heated N_2 by atomic oxygen using the ir tracer method. *The Journal of Chemical Physics*, 59(6):2787–2795, 1973.

[12]W. D. Breshears and P. F. Bird. Effect of oxygen atoms on the vibrational relaxation of nitrogen. *The Journal of Chemical Physics*, 48:4768–4773, 1968.

[13]R.J. McNeal, M.E. Whitson, and G.R. Cook. Quenching of vibrationally excited N_2 by atomic oxygen. *Chemical Physics Letters*, 16(3):507 – 510, 1972.

[14]G. D. Billing. Rate constants and cross sections for vibrational transitions in atom-diatom and diatom-diatom collisions. *Computer physics communications*, 32(1):45–62, 1984.

[15]L. D. Landau. On the theory of transfer of energy at collisions II. *Phys. Z. Sowjetunion*, 2:46–51, 1932.

[16]C. Zener. Non-adiabatic crossing of energy levels. *Proc. R. Soc. Lond.*, A137:696–702, 1932.

[17]E. C. G. Stückelberg. Theory of inelastic collisions between atoms. *Helvetica Physica Acta*, 5:369–423, 1932.

[18]V. Aquilanti, R. Candori, F. Pirani, and Ch. Ottinger. On the dynamics of the vibrationally selective electronic energy transfer from metastable xenon atoms to nitrogen molecules. *Chem. Phys*, 187:171–183, 1994.

[19]F. Pirani, S. Brizi, L. Roncaratti, P. Casavecchia, D. Cappelletti, and F. Vecchiocattivi. Beyond the lennard-jones model: a simple and accurate potential function probed by high resolution scattering data useful for molecular dynamics simulations. *Physical Chemistry Chemical Physics*, 10(36):5489–5503, 2008.

[20]G. D. Billing. The semiclassical treatment of molecular roto-vibrational energy transfer. *Computer Physics Reports*, 1(5):237–296, 1984.

[21]R. W. Hamming. *Numerical methods for scientists and engineers.* New York: Dover Publications, 1986.

[22]P. Gamallo, Miguel González, and R. Sayós. Ab initio derived analytical fits of the two lowest triplet potential energy surfaces and theoretical rate constants for the $N(^4S)+NO(X^2\Pi)$ system. *The Journal of Chemical Physics*, 119(5):2545–2556, 2003.

[23]F. Esposito and I. Armenise. Reactive, inelastic, and dissociation processes in colli-

sions of atomic oxygen with molecular nitrogen. *The Journal of Physical Chemistry A*, 121(33):6211–6219, 2017.

[24]D. Koner, R. J. Bemish, and M. Meuwly. Dynamics on multiple potential energy surfaces: Quantitative studies of elementary processes relevant to hypersonics. *The Journal of Physical Chemistry A*, 124(31):6255–6269, 2020.